

Synthesis of N-Heterocycle Substituted Silyl Ligands within the Coordination Sphere of Iron

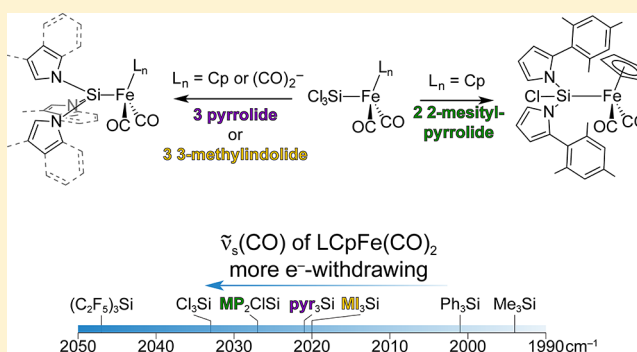
Léon Witteman,[†] Martin Lutz,[‡] and Marc-Etienne Moret^{*,†}

[†]Department of Chemistry, Debye Institute for Nanomaterials Science Utrecht University, Universiteitsweg 99, 3584 CG Utrecht, The Netherlands

[‡]Crystal and Structural Chemistry, Bijvoet Center for Biomolecular Research, Faculty of Science, Utrecht University, Padualaan 8, 3584 CH Utrecht, The Netherlands

Supporting Information

ABSTRACT: N-Heterocycle-substituted silyl iron complexes have been synthesized by nucleophilic substitution at trichlorosilyl ligands bound to iron. The homoleptic (tripyrrolyl)- and tris(3-methylindolyl)silyl groups were accessed from $(\text{Cl}_3\text{Si})\text{CpFe}(\text{CO})_2$ (Cl_3SiFp) by substitution of chloride with pyrrolide or 3-methylindolide, respectively. Analogously, nucleophilic substitution of Cl with pyrrolide on the anionic $\text{Fe}(0)$ synthon $\text{Cl}_3\text{SiFe}(\text{CO})_4^-$ generates the (tripyrrolyl)silyl ligand, bound to the iron tetracarbonyl fragment. The bulkier 2-mesitylpyrrolide substitutes a maximum of 2 chlorides on Cl_3SiFp under the same conditions. The tridentate, trianionic nucleophile tmim (tmimH₃ = tris(3-methylindol-2-yl)methane) proves reluctant to perform the substitution in a straightforward manner; instead, ring-opening and incorporation of THF occurs to form the tris-THF adduct tmim($\text{C}_4\text{H}_8\text{O}$)₃SiFe(CO)₄⁻. The bidentate, monoanionic nucleophile 2-(dipp-iminomethyl)pyrrolide (^{Dipp}IMP, dipp = 2,6-diisopropylphenyl) shows chloride displacement and addition of a second ^{Dipp}IMP moiety on the imine backbone. The heterocycle-based silyl ligands were shown to be sterically and electronically tunable, moderately electron-donating ligands. The presented approach to new silyl ligands avoids strongly reducing conditions and potentially reactive hydrosilane intermediates.



INTRODUCTION

Low-valent silicon(II) compounds are attracting considerable attention as strongly donating, tunable ligands for transition metals.¹ While free silylenes were initially observed as highly reactive intermediates,² the use of nitrogen substituents has given access to a number of persistent silylenes following the first N-heterocyclic silylene (NHSi) reported in 1994 by Denk et al.³ Similarly to N-heterocyclic carbenes (NHC), stable silylenes bind a variety of transition metals.^{4–6} However, owing to the lower electronegativity and larger size of silicon, they conserve a higher Lewis acidity than their carbon-based congeners and they are often stabilized by coordination of a Lewis base, resulting in a 4-coordinate Si(II) center in the metal complex.^{4,7,8} The coordination chemistry of Si(II) ligands has now been well established, and their use as supporting ligands in catalysis is emerging as a promising area of research.^{1,8–16}

In contrast with their neutral congeners, anionic Si(II) ligands (silyl anions or silanides) have seen less applications as supporting ligands,^{17–20} their use being mostly limited to multidentate architectures,²¹ including a recently reported PSiP pincer system featuring indolyl linkers.²² This presumably arises from the high reactivity of the metal–silicon bond, exemplified by the role of metal–silyl complexes as reactive intermediates in catalytic hydrosilylation.^{8,23–25} A possible approach

toward stable silanides is the use of electron-withdrawing substituents to tame the reducing strength of the Si-centered lone pair. Encouragingly, this approach has allowed for the isolation of free silanides bearing trimethylsilyl and aromatic^{26–30} moieties, and more recently fluoroalkyl³¹ and pyrazole moieties.³² In this context, silyl ligands bearing electron-withdrawing N-heterocyclic substituents such as N-pyrrolyl or N-indolyl represent an attractive yet underexplored ligand class, with only a handful of representatives known to date.³³

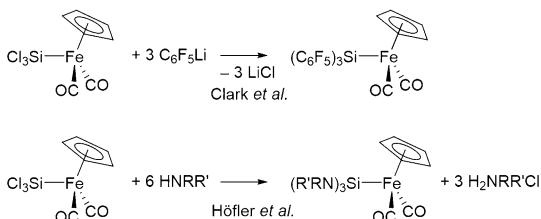
The three classical approaches for the synthesis of silanides are deprotonation of an Si–H bond, nucleophilic cleavage of a Si–Si bond with an alkoxide, and reduction of (1) a silicon-halogen, (2) a disilane, or (3) a Si–Ar bond.^{27,30,32,34} Relatively harsh reaction conditions³⁵ and possible side reactions³⁶ (e.g., substitution at Si by strong bases³⁷) limit the scope of these reactions. Therefore, many compounds containing metal–silicon bonds are not prepared by coordination of a free silanide but rather by oxidative addition of an Si–H bond to a reduced metal precursor.^{38–40} In particular, the only tris(N-pyrrolyl)silyl complexes known prior to this work have been synthesized by oxidative addition of tris(N-pyrrolyl)silane

Received: June 11, 2018

Published: September 10, 2018

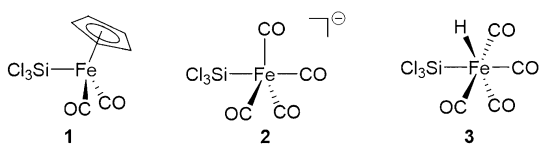
to Os and Ru.⁴¹ An interesting alternative to these routes is substitution at a metal-bound silyl moiety bearing one or more good leaving groups, typically halogens. Following the initial report of nucleophilic substitution of chloride with dimethylamine to obtain *trans*-ClPt(PEt₃)₂SiH₂NMe₂,⁴² this methodology was previously applied to the exchange of Cl on Cp(CO)₂Fe^{II}SiCl₃ (FpSiCl₃) for pentafluorophenyl⁴³ and amido (R'RN⁻)^{44,45} substituents (Scheme 1). It has also been used for simple silyl group transformations on Ni⁴⁶ and other group 6–8 transition metals.^{46–54}

Scheme 1. Nucleophilic Substitution of –Cl with –C₆F₅ and –R'RN in (Cl₃Si)CpFe(CO)₂^{43,44}



Here we investigate the synthesis of a range of unusual silyl ligands incorporating pyrrolyl and indolyl substituents by nucleophilic substitution on the Fe-bound SiCl₃ fragment. Constructing complex silyl ligands in the coordination sphere of the metal avoids the intermediacy of hydrosilanes—which can be subject to undesired rearrangements^{55–61}—and reactive silanides. We show that such substitution reactions are possible both on the neutral Fe(II) complex Cl₃Si–FeCp(CO)₂ (**1**) and on the Fe(0) anion Cl₃Si–Fe(CO)₄⁻ (**2**), the latter being conveniently generated by deprotonation of the corresponding neutral Fe(II) hydride (**3**, Chart 1). Steric bulk can

Chart 1. Chlorosilyl Iron Complexes Used as Precursors for Nucleophilic Substitution



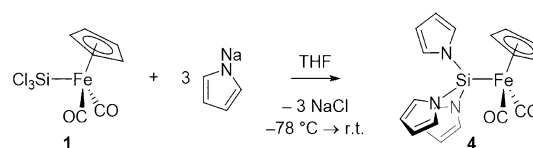
be incorporated around silicon in this way, and we characterize two more complex reactions occurring with multidentate nucleophiles to form cyclic silyl derivatives. The electronic properties of the obtained silyl ligands are discussed on the basis of NMR and IR spectroscopy.

RESULTS AND DISCUSSION

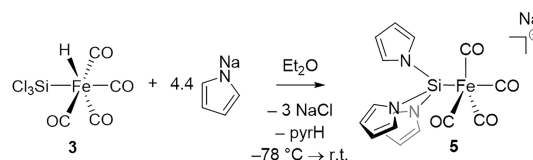
In a first set of experiments, the transformation of the trichlorosilyl ligand into tris(N-pyrrolyl)silyl was investigated. Complete substitution was achieved on the Fe(II) complex Cl₃Si–FeCp(CO)₂ **1**: reaction with 3 equiv sodium pyrrolide produced the trisubstituted complex **4** (Scheme 2) resulting in a diagnostic shift of the ²⁹Si NMR resonance from 63.4 to 39.1 ppm. Trisubstitution is evident from the ratio of integrals between the Pyr–H, and the C₅H₅ ¹H NMR resonances.

In addition, the anionic tris(pyrrolyl)silyl complex Na-**5** was accessed by addition of a solution of the hydride complex **3** to 4 equiv sodium pyrrolide in Et₂O at –78 °C (Scheme 3). Detection of the anionic product by electrospray ionization mass spectrometry (ESI-MS) is straightforward (M⁻: *m/z* =

Scheme 2. Nucleophilic Substitution of Chloride with Pyrrolide on Compound 1



Scheme 3. Nucleophilic Substitution of Chloride with Pyrrolide on the Iron Tetracarbonyl Complex



393.9943 au, calc'd *m/z* = 393.9947 au). The absence of an Fe–H resonance in the ¹H NMR spectrum indicates that deprotonation has taken place, i.e. the fourth equiv of pyrrolide functions as a sacrificial base for deprotonation of **3** to Na-**2**. Additionally, the disappearance of the three distinct ¹³C NMR resonances around 200 ppm for **3**⁶² and appearance of a single resonance at 217.9 ppm for Na-**5** is consistent with the formation of a fluxional 5-coordinate structure with fast axial–equatorial exchange.^{63–73} The independently synthesized ammonium salt NEt₄-**2**⁷⁴ readily undergoes substitution under the same conditions, showing that nucleophilic substitution is feasible on Cl₃Si bound to Fe(0) and may take place after deprotonation of **3**. From a practical point of view, however, reactions involving NEt₄-**2** are less well-behaved because the counterion is susceptible to Hoffman degradation, i.e. 1,2-elimination to give NEt₃, ethylene, and pyrH.

Crystals of Na-**5** suitable for X-ray crystallography were grown by slow diffusion of hexane into a solution of the complex in the presence of benzo-15-crown-5 in THF. The X-ray crystal structure reveals a trigonal bipyramidal (TBP) geometry with the –SiPyr₃ moiety in the apical position, as commonly found for analogous phosphine,⁷³ (base stabilized) silylene,^{7,75–94} and silyl^{89,95,96} iron tetracarbonyl complexes (Figure 1). The Si–Fe distance in **5** (2.2576(8) Å) is well in between the extremes, close to the mean for silyl and silylene iron

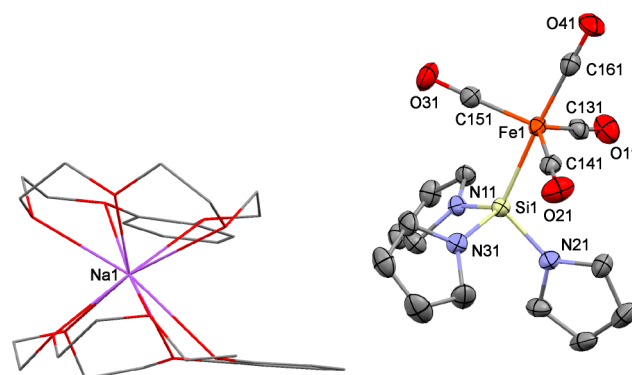
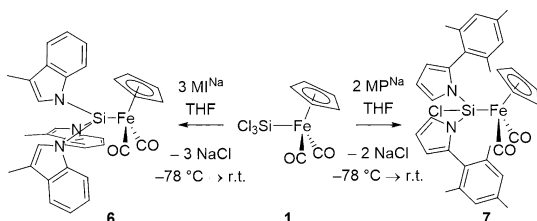


Figure 1. Molecular structure of Na-**5** in the crystal. Ellipsoids at 50% probability. Hydrogen atoms were omitted and the counterion shown as wireframe for clarity. Selected bond lengths (Å) and angles (deg): C151–O31 1.159(3), C161–O41 1.141(3), C131–O11 1.160(3), C141–O21 1.147(3), Fe1–Si1 2.2576(8), Si1–N11 1.771(2), Si1–N21 1.774(2), Si1–N31 1.777(2), N11–Si1–N21 103.21(11), N21–Si1–N31 100.70(11), N31–Si1–N11 99.67(10).

tetracarbonyl complexes ($2.1960^{86} < \text{Si-Fe} < 2.3630(8)^{93}$ ($\text{Si-Fe} = 2.2663 \text{ \AA}$) and, more generally, of Si-Fe bonds.³⁹ The single precedent of a structurally characterized pyr_3Si -containing complex is $\text{Os}(\text{SiPyr}_3)\text{H}(\text{CO})_2(\text{PPh}_3)_2 \cdot \text{H}_2\text{O}$ reported by Hübler et al.⁴¹ In this complex, both the N-Si-N angles and the Si-M distance are very similar to those in Na-5 (see ESI Table S1). The difference in Si-M distance between the two complexes (0.117 Å) is the same as the difference in covalent radius of iron and osmium (0.12 Å).⁹⁷

The generality of this substitution for other monodentate heterocycles was investigated. The substitution of chloride with 3-methylindolide (MI) on **1** afforded the trisubstituted **6** (Scheme 4), as indicated by a 3:1 ratio of the ¹H NMR

Scheme 4. Nucleophilic Substitution with 3-Methylindolide (left) and 2-Mesitylpyrrolide (right) on **1**



resonance integrals of MI with those of the Cp ligand. In contrast, substitution of chloride with the bulkier 2-mesitylpyrrolide (MP) on **1** affords the disubstituted **7** (Scheme 4), the structure of which was further confirmed by X-ray crystal structure determination (Figure 2). The solid-state structure reveals a

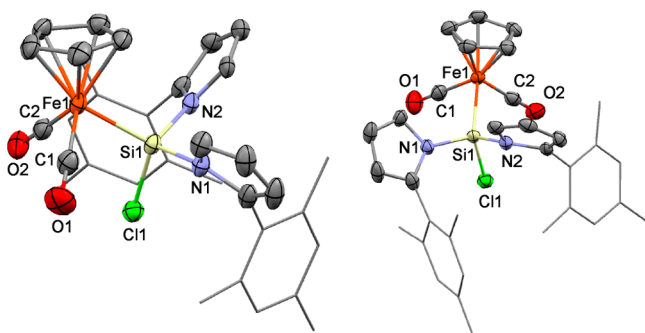


Figure 2. Two views of the molecular structure of **7** in the crystal. Ellipsoids at 50% probability. Hydrogen atoms were omitted and mesityl residues shown as wireframe for clarity. Selected bond lengths (Å) and angles (deg): C1–O1 1.143(4), C2–O2 1.143(4), Fe1–Si1 2.2721(10), Si1–Cl1 2.0627(13), Si1–N1 1.787(3), Si1–N2 1.781(3), N1–Si1–Cl1 106.10(10), N1–Si1–N2 103.00(12), N2–Si1–Cl1 105.11(10).

piano-stool complex with the silyl ligand as one of the legs. Compared to Na-5, the Si-Fe distance is slightly longer ($\Delta d = 0.0145(13) \text{ \AA}$) and the angle sum of the substituents on silicon is significantly bigger ($314.21(19)$ vs $303.58(18)^\circ$). In solution, compound **7** exhibits three ¹H NMR resonances in a 1:1:1 ratio for the individual methyl-groups on the equivalent mesityl moieties, arising from slow rotation around the $\text{C}_{\text{aryl}}-\text{C}_{\text{pyr}}$ bonds. The energy barriers for interchanging the methyl groups through rotation around the Si-Fe bond and the $\text{C}_{\text{aryl}}-\text{C}_{\text{pyr}}$ bonds were calculated in the gas phase by DFT potential energy surface scan (PES) calculations (see ESI Figures S1–S4).⁹⁸ These calculations show a maximum energy difference of about

8 kcal/mol upon 360° rotation around the Si-Fe bond and of at least 33 kcal/mol upon 180° rotation around either $\text{C}_{\text{aryl}}-\text{C}_{\text{pyr}}$ bond. This corroborates the interpretation of the NMR spectrum in terms of a fast rotation around the Si-Fe bond, rendering the mesityl groups equivalent on the NMR time-scale, with magnetically inequivalent methyl groups within a mesityl moiety.

The series of complexes described herein provides an opportunity to study the effect of substitution on the properties of silyl ligands (Table 1). Formal substitution of three

Table 1. ²⁹Si NMR (ppm), IR $\tilde{\nu}(\text{CO})$ (cm^{-1}), Crystallographic Si-Fe Distance (Å) and the Sum of E-Si-E Angles (deg, E = Cl, N) of All Compounds

Compound	δ (Si)	$\tilde{\nu}(\text{CO})$	Si-Fe	$\Sigma(\text{E-Si-E})$
Fp-SiCl ₃ (1)	63.4	2033, 1985		
$[(\text{CO})_4\text{Fe-SiCl}_3]^-$ (2) ⁸⁹	67.8	2026, 1941, 1917	2.237(3)	304.8(2)
Fp-SiPyr ₃ (4)	39.1	2021, 1970		
$[(\text{CO})_4\text{Fe-SiPyr}_3]^-$ (5)	45	2019, 1934, 1906	2.2576(8)	303.58(18)
Fp-Si(MI) ₃ (6)	32.4	2020, 1969		
Fp-SiCl(MP) ₂ (7)	42.6	2027, 1977	2.2721(10)	314.21(19)

chlorides in compound **1** with three pyrrolides in **4** results in a slight shift of the IR bands $\tilde{\nu}_s(\text{CO})$ and $\tilde{\nu}_a(\text{CO})$ to lower energies by 12 and 15 cm^{-1} , respectively, indicating that the $\text{pyr}_3\text{Si-}$ ligand is slightly more electron donating than the $\text{Cl}_3\text{Si-}$ analogue. Similarly, the three IR bands associated with CO stretch modes of the $\text{Fe}(\text{CO})_4$ moiety shift slightly from 2026, 1941, and 1917 cm^{-1} in the $\text{Cl}_3\text{Si-}$ complex **2** to 2019, 1934, and 1906 cm^{-1} in the $\text{Pyr}_3\text{Si-}$ complex **5**. The IR absorptions in the tris(3-methylindolyl)silyl complex **6** are within 1 cm^{-1} of those of the tris-pyrrolysilyl complex **4**, indicating that the net electronegativity of pyr and MI is virtually the same. The $\tilde{\nu}(\text{CO})$ bands of the dipyrrolide, monochloride complex **7** (2027, 1977 cm^{-1}) are found between those of **1** (2033, 1985 cm^{-1}) and **4** (2021, 1970 cm^{-1}), consistent with intermediate electronic properties between $\text{Cl}_3\text{Si-}$ and $\text{Pyr}_3\text{Si-}$. More generally, the heterocycle silyl ligands in **4**, **6**, and **7** are less donating than $\text{Ph}_3\text{Si-}$ and $\text{Me}_3\text{Si-}$ (2001, 1994 cm^{-1} , respectively) and more donating than $(\text{C}_2\text{F}_5)_3\text{Si-}$ and $\text{Ph}_3\text{P-}$ (2047, 2057 cm^{-1} , respectively) in the corresponding CpFe-(CO)₂ complexes (Figure 3).

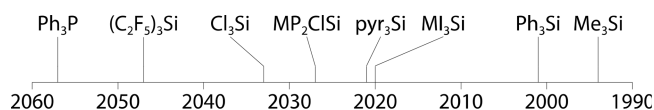


Figure 3. Graphical representation of highest $\tilde{\nu}(\text{CO})$ of $\text{LCpFe}(\text{CO})_2$ in cm^{-1} .

As was observed from the effect on $\tilde{\nu}(\text{CO})$, substitution of chloride with pyrrolides increases the overall donor strength of the ligand, which generally arises from a combination of increased σ -basicity and/or decreased π -acidity. Interestingly, the stronger donor Pyr_3Si displays a longer Si-Fe(CO)₄ bond in compound Na-5 than Cl_3Si in **2** by 0.021(3) Å. This lengthening indicates a slightly weaker bond, suggesting that π -acidity is important to the Fe-Si bonding in this series of compounds.

The sum of the R-Si-R substituent angles around silicon is found to be less sensitive to the electronegativity of the substituent. Generally speaking, these angles provide a measure for

the extent of hybridization of the bonding orbitals: smaller R–Si–R angles indicate more p-character in the Si–R bonding orbitals and consequently more s-character in the Si–M bonding orbital, according to Bent's rule.⁹⁹ In the ideal case, the sum of angles is 328.5° for sp³ hybridization and 270° for the nonhybridized extreme. The sums of the E–Si–E angles in Na-5 (303.58(18)°) and 2 (304.8(2)°) are virtually equal but significantly lower than that of the C–Si–C angles in Me₃SiFe(CO)₄[−] (310.8(15)°),⁹⁶ indicating that electron withdrawing substituents on silicon result in a higher s-character of the σ-bonding orbital. Interestingly, the angles between the substituents on silicon in Fp-based 7 are slightly larger (103–106°) than those in Fe(CO)₄-based Na-5 (100–103°), suggesting more p-character in the Si–M bonding orbitals and, hence, a less ionic Si–M bond, likely because of the stronger electron-accepting character of the Fe(II) fragment compared to the Fe(0) fragment in Na-5.

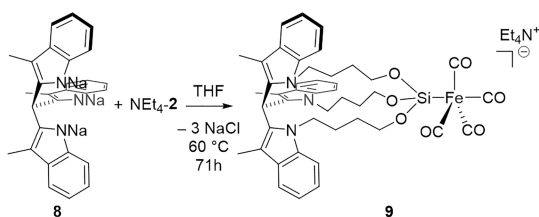
The ²⁹Si NMR signals in Table 1 generally shift toward high field upon substitution of chloride with pyrrolide. Interestingly, the high-field shift observed upon trisubstitution is almost identical on the Fp and Fe(CO)₄ fragments: 24 ppm difference between 1 and 4 vs 23 ppm difference between 2 and 5. However, the series of Fp complexes (4, 6, 7) exhibit no straightforward correlation with the donor strength of the ligand: the difference in chemical shift between trisubstituted 4 and disubstituted 7 (Δδ = 3.5 ppm) is smaller than that between 4 and the tris-indolyl substituted 6 (Δδ = 6.7 ppm), whereas 4 and 6 exhibit indistinguishable donor properties according to $\bar{z}(\text{CO})$. Such nonlinearity was also observed by Leis et al.⁷⁹ for a range of HMPA stabilized silylene metal carbonyl complexes (M = Fe, Cr, Ru; R in SiR₂ = *t*BuO, *t*BuS, Me, Cl, 1-AdaO, 2-AdaO, NeopO, TritO, Ph). This behavior has been attributed to a combined influence of diamagnetic and paramagnetic effects on the silicon shift.¹⁰⁰

Overall, the spectroscopic data consistently indicate that pyrrolide and indolide substituents on silicon are electron withdrawing, only slightly less so than chloride, resulting in moderately donating silyl groups. Furthermore, their effect on the electronic properties of the silyl ligand is approximately the same for an anionic Fe(0) and a neutral Fe(II) supporting metal. This suggests that such heterocycles might be used to construct tunable analogues of the SiCl₃ ligand by varying the substitution patterns on the heterocycles.

MULTIDENTATE N-DONORS

Having established the substitution at silicon for simple pyrrolide derivatives, the reactivity of multidentate nucleophiles was investigated, starting with the trisodium salt of tris(3-methylindol-2-yl)methane (tmimNa₃, 8, Scheme 5). The tmim scaffold has previously been shown to form stable phosphine ligands that can be bound to Fe(CO)₄.⁷³ Additionally, we

Scheme 5. Nucleophilic Substitution of Chloride and Incorporation of THF on 2



recently showed that the tmim^{3−} trianion can fully substitute the Si(II) center in (Idipp)SiCl₂ (Idipp = 2,3-dihydro-1,3-bis(2,6-diisopropylphenyl)-1H-imidazol-2-ylidene) to form the naked silanide (tmim)Si[−].³³ Scaffold tmimH₃ was synthesized according to the literature procedure,¹⁰¹ followed by deprotonation using NaH. The reaction of 8 with NEt₄-2 was initially conducted in THF at 60 °C. Under these conditions, the targeted trisubstitution product could not be detected. In contrast, analysis of the reaction mixture by ESI-MS indicates the presence of an anionic complex incorporating three additional THF molecules at M[−] = 812.2437 au (Figure 4).

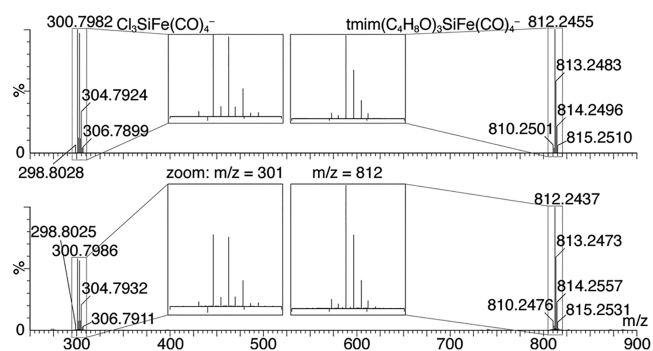


Figure 4. ESI-MS of 9 in THF after reaction for 65 h at 60 °C in THF; calculated (top), experimental (bottom). Insets: enlarged isotope patterns of the designated peaks.

Interestingly, signals corresponding to the incorporation of one or two THF molecules were not observed, whereas the unsubstituted complex is still present, suggesting that the second and third incorporation of THF are much faster than the first. The corresponding product could unfortunately not be fully isolated but could be sufficiently enriched to a purity of approximately 70% to be analyzed by multinuclear NMR (*vide infra*), confirming its identity as the product of triple ring-opening and insertion of THF, compound 9 (Scheme 5). In other solvents, the reaction of NEt₄-2 and 8 gave unresolved complex mixtures. Additionally, reaction between the neutral precursor 1 and 8 afforded an intractable mixture of products.

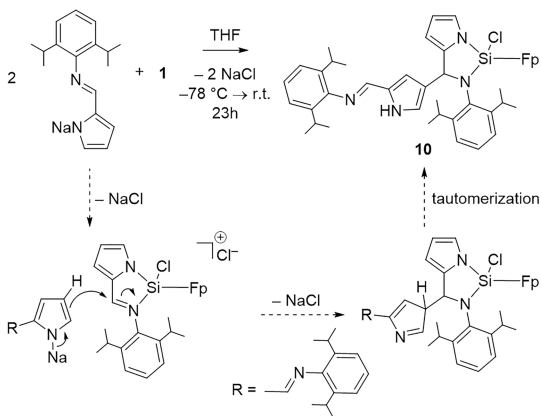
The tmim moiety of crude product 9 in CD₃CN gives rise to four resonances in ¹H NMR for the aromatic protons, indicating local 3-fold symmetry (see Supporting Information Figure S15). Furthermore, the spectrum of the reaction mixture of 9 displays four multiplet signals at δ = 3.66, 3.73, 4.00, and 4.10 ppm which couple in HMQC with two signals in ¹³C NMR at 44.5 and 61.9 ppm, originating from the diastereotopic protons of N–CH₂ and O–CH₂. An additional set of three multiplets with a 1:2:1 ratio at δ = 1.60, 1.77, and 2.34 ppm, corresponding to four protons, and coupling with two signals in ¹³C NMR at 29.1 and 30.7 ppm, originates from the central CH₂ moieties.

We propose that 9 forms through a ring-opening reaction of THF by nucleophilic attack of 8 on the THF α-carbon, presumably preceded by coordination of THF to silicon, making its α-carbon more prone to nucleophilic attack. A related ring opening and incorporation of THF has previously been observed by Okazaki et al.¹⁰² in the reaction between ClSiMe₂NR₂ and the Fp-anion to form Fp(CH₂)₄OSiMe₂NR₂. They explain this by initial coordination of THF to the silane, followed by nucleophilic attack of Fp[−] on the α-carbon. Similarly, Dufour et al.¹⁰³ observed ring opening and incorporation of THF in a reaction between the chlorosilyliron complex

ClSiR_2Fp ($\text{R}_2 = -\text{CH}_2\text{CH}=\text{CHCH}_2-$) and the Fp anion, resulting in a $\text{FpSiR}_2\text{O}(\text{CH}_2)_4\text{Fp}$ complex. They suggest substitution of chloride in FpSiR_2Cl with THF to give an oxonium species followed by nucleophilic attack of Fp^- on the α -carbon. The transformation of **8** to **9** shows that multiple insertions are also possible with a suitable multidentate organic nucleophile.

Finally, the monoanionic bidentate iminopyrrolide substituent $\text{D}^{\text{ipp}}\text{IMP}$ was investigated as a nucleophile (Scheme 6).

Scheme 6. Reaction of $\text{D}^{\text{ipp}}\text{IMP}$ with **1** in THF at $-78^\circ\text{C} \rightarrow \text{r.t.}$, Including Proposed Reaction Pathway^a



^aFp = $\text{Cp}(\text{CO})_2\text{Fe}$.

As the imine functionality in $\text{D}^{\text{ipp}}\text{IMP}$ is susceptible to intramolecular hydrosilylation, the corresponding hydrosilanes are unsuitable precursors for silyl complexes via either deprotonation or oxidative addition.⁵⁷ $\text{D}^{\text{ipp}}\text{IMP}$ was synthesized according to the literature procedure,¹⁰⁴ followed by deprotonation using NaHMDS . Reaction of either two or three equiv of $\text{D}^{\text{ipp}}\text{IMPNa}$ with **1** formed the same compound **10**, while reaction of 1 equiv of $\text{D}^{\text{ipp}}\text{IMPNa}$ with **1** afforded a mixture of compounds containing both **1** and **10**. The ^{29}Si NMR resonance of **10** is found at $\delta = 39.4$ ppm, similar to complexes **4**, **6**, and **7** (Table 1), consistent with substitution at Si taking place. ^1H NMR analysis of **10** indicates that two $\text{D}^{\text{ipp}}\text{IMP}$ molecules have been incorporated and that the reaction is more complex than simple disubstitution at silicon. The ^1H NMR spectrum displays five distinct signals for the pyrrole moieties. A COSY spectrum indicates the presence of two distinct pyrrole rings, one with a 3H spin system ($^3J(\text{H,H}) = 2.8$ Hz, $^4J(\text{H,H}) = 1.3$ Hz) and one with a 2H spin system (broad singlets). The weak coupling in the latter suggests at least $^4J(\text{H,H})$ -coupling between them. Moreover, both spin systems are in a 1:1 ratio with the Cp group, indicating the presence of 2 pyrrole moieties for one metal center. Interestingly, the presence of a resonance at $\delta = 9.63$ ppm suggests that the product contains an N–H bond. Finally, a singlet resonance in ^1H NMR at $\delta = 5.75$ ppm accounting for 1H and coupling with an sp^3 -carbon at $\delta = 61.9$ ppm indicates the presence of an sp^3 -CHN fragment. The data outlined above collectively support the assignment of **10** as the C–C coupled structure depicted in Scheme 6. The *i*Pr residues give rise to 3 septets in a 1:1:2 ratio and 5 doublets in a 1:1:1:1:4 ratio, suggesting hindered rotation around the $\text{C}_{\text{aryl}}\text{--N}_{\text{amine}}$ bond and free rotation around the $\text{C}_{\text{aryl}}\text{--N}_{\text{imine}}$ bond. In ^{13}C NMR two resonances appear for the carbonyl carbons, which suggests that the substituent is bound to silicon in a bidentate fashion, rendering the silicon

atom chiral and hence the carbonyls diastereotopic. The structure inferred from NMR was confirmed by the crystal structure (Figure 5). Crystals suitable for X-ray crystallography were

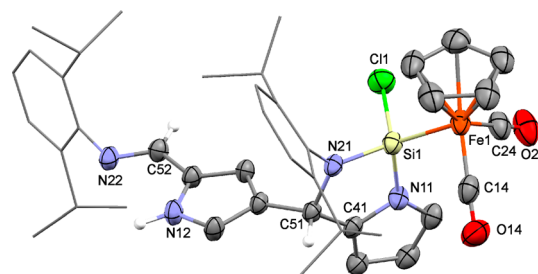


Figure 5. Molecular structure of **10** in the crystal. Ellipsoids at 50% probability. Hydrogen atoms and cocrystallized hexane were omitted and diisopropylphenyl residues shown as wireframe for clarity. Selected bond lengths (Å) and angles (deg): Fe1–Si1 2.2456(7), C14–O14 1.141(3), C24–O24 1.146(3), Si1–Cl1 2.1144(9), Si1–N11 1.761(2), Si1–N21 1.724(2), N21–C51 1.493(3), N22–C52 1.275(3), N21–Si1–N11 91.40(9), N11–Si1–Cl1 102.31(7), N21–Si1–Cl1 110.73(7).

grown by slow diffusion of hexane into a THF solution. The N–Si distance is smaller for the former imine (N21–Si) than for the pyrrole substituent (N11–Si), likely due to hyperconjugation of the N21 lone pair into Si, as opposed to N11, where the lone pair is delocalized in the aromatic system. The sum of E–Si–E angles ($304.44(13)^\circ$) is small compared to **7**, due to the 5-membered ring system. As a result, the amount of *s*-character in the Si–Fe bond is higher, resulting in a shorter distance (**10**: 2.2456(7), **7**: 2.2721(10) Å).

The formation of complex **10** is consistent with initial substitution of two chlorides by one $\text{D}^{\text{ipp}}\text{IMP}$, forming an overall cationic complex bearing an iminopyrrolide chlorosilylene ligand (Scheme 6). Activation of the imine through coordination to the electron-poor silicon would then facilitate nucleophilic attack of a second $\text{D}^{\text{ipp}}\text{IMP}$ anion. The preference for the 4-position is likely sterically driven. The formation of **10** is kinetically competitive with that of the intermediate, preventing isolation of the latter.

CONCLUSIONS

A series of unusual silyl-iron complexes with N-heterocyclic substituents was synthesized by nucleophilic substitution of the chlorides of a metal-bound trichlorosilyl ligand. This method affords homoleptic silyl ligands with unencumbered substituents such as pyrrol-1-yl (pyr_3Si^-) and 3-methylindol-1-yl ($(\text{MI})_3\text{Si}^-$), and the heteroleptic silyl ligand $(\text{MP})_2\text{ClSi}^-$ with the bulkier 2-mesitylpyrrol-1-yl. The ligands were found to be slightly more electron-donating than Cl_3Si^- , which makes them moderately electron donating and electronically and sterically tunable. Attempts to expand this methodology to multidentate nucleophiles (tmim, $\text{D}^{\text{ipp}}\text{IMP}$) led to more complex reactivity pathways. These results demonstrate that on-metal synthesis can be applied to the preparation of silyl ligands of increased complexity, allowing for fine-tuning of their steric and electronic properties.

EXPERIMENTAL SECTION

All reactions involving silicon-containing compounds were conducted under an N_2 atmosphere by using standard glovebox or Schlenk techniques. Diethyl ether, *n*-hexane, toluene, and acetonitrile were dried with an MBRAUN MB SPS-79 system, degassed by bubbling

with N₂ for 30 min, and stored over molecular sieves in a glovebox. THF was distilled from benzophenone/Na, degassed by bubbling with N₂ for 30 min, and stored over molecular sieves in a glovebox. All chemicals were obtained commercially and used as received unless stated otherwise. All NMR chemical shifts are reported relative to TMS with the residual solvent signal as internal standard.¹⁰⁵ All NMR experiments involving silicon-containing compounds were conducted in J-Young NMR tubes under an N₂ atmosphere. IR spectra were recorded on a PerkinElmer Spectrum Two FT-IR spectrometer. ESI-MS measurements were performed on a Waters LCT Premier XE KE317 spectrometer. Elemental analysis was conducted by the Mikroanalytisches Laboratorium Kolbe. Ph₄PfCl was dried according to the method described in purification of laboratory chemicals.¹⁰⁶ The following compounds were synthesized according to literature procedures: Cl₃SiFe(H)(CO)₄ (**3**),^{38,107} NEt₄[Cl₃SiFe(CO)₄]₄ (**2**),⁷⁴ Cl₃SiCpFe(CO)₂ (**1**),^{53,108,109} DIPPIMPf, ¹⁰⁴ (tmim)₃ (**8**).¹⁰¹

Computational Methods. Calculations were performed using Gaussian09, Revision D.01.⁹⁸ All structures were optimized using the TPSS functional with the TZVP basis set. The absence of imaginary frequencies was confirmed for all structures. On the optimized geometries, potential energy surface scans were conducted using the Modredundant method implemented in Gaussian09.

Syntheses. *Synthesis of (pyr₃Si)CpFe(CO)₂ (**4**).* A precooled THF (1 mL) solution of **1** (39 mg, 0.13 mmol) was added to a precooled THF (4 mL) solution of sodium pyrrolide (33 mg, 0.37 mmol) at -78 °C. The vial was rinsed with THF (1 mL) and the solution added to the mixture, which was allowed to warm to r.t. over 20 h. The solvent was evaporated, toluene (2 mL) was added to the residue, and the solvent was evaporated again to remove most of the residual THF. The mixture was extracted with toluene (2 × 2 mL) and the solvent was removed *in vacuo*. Analytically pure material (44 mg, 0.11 mmol, 87%) was obtained by precipitation from toluene (2 mL) with hexane (12 mL), storage at -35 °C for 20 h and removal of the supernatant. ¹H NMR (400 MHz, C₆D₆, 25 °C) δ = 6.80 (t, ²J(H,H) = 2.0 Hz, ³J(H,H) = 2.0 Hz, 6H, pyrrole-H α), 6.44 (t, ²J(H,H) = 2.0 Hz, ³J(H,H) = 2.0 Hz, 6H, pyrrole-H β), 3.89 ppm (s, 5H); ¹³C NMR (101 MHz, C₆D₆, 25 °C) δ = 212.4 (CO), 124.5 (pyrrole), 112.4 (pyrrole), 84.6 ppm (Cp); ²⁹Si NMR (79 MHz, C₆D₆, 25 °C) δ = 39.1 ppm; IR (THF): $\tilde{\nu}$ = 2021, 1970 cm⁻¹; Anal. Calc'd C₁₉H₁₇FeN₃O₂Si: C 56.59, H 4.25, N 10.42%; found C 56.57, H 4.29, N 10.37.

*Synthesis of [(pyr₃Si)Fe(CO)₄]⁻Na⁺ (**Na-5**).* A Et₂O (6 mL) solution of **3** (96 mg, 0.32 mmol) was added dropwise to a precooled suspension of NaPyr (127 mg, 1.44 mmol) in Et₂O (5 mL) at -79 °C, resulting in a pink solution. The mixture was allowed to warm to r.t. and was stirred for another 15 min, during which a white precipitate formed. Removal of the precipitate by filtration and concentration *in vacuo* afforded a pink powder (102 mg, 0.26 mmol, 77%). Crystals suitable for X-ray crystallography were grown by slow diffusion of hexane into a concentrated solution of **5** in THF in the presence of benzo-15-crown-5. ¹H NMR (400 MHz, C₆D₆ + C₄H₈O, 25 °C): δ = 7.13 (t, ²J(H,H) = 2.0 Hz, ³J(H,H) = 2.0 Hz, 6H, pyrrole-H α), 6.36 ppm (t, ²J(H,H) = 2.0 Hz, ³J(H,H) = 2.0 Hz, 6H, pyrrole-H β); ¹³C NMR (101 MHz, C₆D₆ + C₄H₈O, 25 °C) δ = 217.9 (CO), 125.5 (pyrrole), 110.5 ppm (pyrrole); ²⁹Si NMR (79 MHz, C₆D₆ + C₄H₈O, 25 °C) δ = 45.0 ppm; ESI-MS: M⁻: m/z = 393.9943 au, calc'd m/z = 393.9947 au; IR (THF): $\tilde{\nu}$ = 2019m, 1934m, 1906s cm⁻¹; The presence of solvation THF in the solid hampered the determination of anal., which was therefore determined on the crystallized (benzo-15-crown-5)₂Na salt: Anal. Calc'd C₄₄H₅₂FeN₃NaO₁₄Si: C 55.41, H 5.50, N 4.41%; found C 55.12, H 5.61, N 4.51%.

X-ray Crystal Structure Determination of Na-5. [C₂₈H₄₀NaO₁₀]⁻[C₁₆H₁₂FeN₃O₄Si], Fw = 953.81, colorless needle, 0.40 × 0.10 × 0.06 mm³, monoclinic, P2₁/c (no. 14), a = 14.3159(8), b = 10.3810(4), c = 30.5866(18) Å, β = 90.911(1)°, V = 4545.0(4) Å³, Z = 4, D_x = 1.394 g/cm³, μ = 0.44 mm⁻¹. The diffraction experiment was performed on a Bruker Kappa ApexII diffractometer with sealed tube and Triumph monochromator (λ = 0.71073 Å) at a temperature of 150(2) K up to a resolution of (sin θ/λ)_{max} = 0.65 Å⁻¹. The crystal appeared to be twinned with a 2-fold rotation about *hkl* = (0,0,1) as

twin operation. Consequently, two orientation matrices were used for the integration with the Eval15 software.¹¹⁰ This resulted in a total of 90621 measured reflections. A multiscan absorption correction and scaling was performed with TWINABS¹¹¹ (correction range 0.53–0.75). 10744 Reflections were unique (R_{int} = 0.076), of which 8267 were observed [*I* > 2 σ (*I*)]. The structure was solved with Patterson superposition methods using SHELXT.¹¹² Least-squares refinement was performed with SHELXL-2014¹¹³ against F² of all reflections. Non-hydrogen atoms were refined freely with anisotropic displacement parameters. Hydrogen atoms were introduced in calculated positions and refined with a riding model. 578 Parameters were refined with no restraints. R1/wR2 [*I* > 2 σ (*I*)]: 0.0448/0.0988. R1/wR2 [all refl.]: 0.0706/0.1090. S = 1.023. Twin fraction BASF = 0.1904(6). Residual electron density between -0.26 and 0.45 e/Å³. Geometry calculations and checking for higher symmetry was performed with the PLATON program.¹¹⁴

*Synthesis of [(Ml)₃Si]CpFe(CO)₂ (Ml = 3-methylindolyl, **6**).* A precooled THF (1 mL) solution of **1** (52 mg, 0.17 mmol) was added to a precooled THF (4 mL) solution of sodium 3-methylindolide (Ml^{Na}, 111 mg, 0.500 mmol) at -78 °C. The flask was rinsed with THF (1 mL) and the solution added to the mixture, which was allowed to warm to r.t. and stirred for 20 h. The solvent was evaporated, toluene (2 mL) was added to the residue, and the solvent was evaporated again to remove most of the residual THF. The mixture was extracted with toluene (2 × 2 mL) and the solvent was removed *in vacuo*. Analytically pure material (90 mg, 0.15 mmol, 91%) was obtained by trituration of the solid with hexane (2 mL) and drying *in vacuo*. ¹H NMR (400 MHz, C₆D₆, 25 °C): δ = 7.54 (ddd, ³J(H,H) = 7.8 Hz, ⁴J(H,H) = 1.3 Hz, ⁵J(H,H) = 0.8 Hz, 3H, indole-H7), 7.46 (dt, ³J(H,H) = 8.3 Hz, ⁴J(H,H) = 0.9 Hz, 3H, indole-H4), 7.19 (q, ⁴J(H,H) = 1.0 Hz, 3H, indole-H2), 7.10 (ddd, ³J(H,H) = 7.9 Hz, ³J(H,H) = 7.1 Hz, ⁴J(H,H) = 1.0 Hz, 3H, indole-H6), 6.98 (ddd, ³J(H,H) = 8.4 Hz, ³J(H,H) = 7.1 Hz, ⁴J(H,H) = 1.3 Hz, 3H, indole-H5), 3.79 (s, 5H, Cp), 2.18 ppm (d, ⁴J(H,H) = 1.2 Hz, 9H, CH₃). ¹³C NMR (101 MHz, C₆D₆, 25 °C): δ = 213.5 (CO), 141.0, 133.2, 122.8, 121.1, 119.6, 115.8, 115.1, 84.9 (Cp), 10.0 ppm (CH₃); ²⁹Si NMR (79 MHz, C₆D₆, 25 °C) δ = 32.4 ppm; IR (THF): $\tilde{\nu}$ = 2020, 1969 cm⁻¹; Anal. Calc'd C₃₄H₂₉FeN₃O₂Si: C 68.57, H 4.91, N 7.06%; found C 68.22, H 5.27, N 6.74%.

*Synthesis of [(MP)₂ClSi]CpFe(CO)₂ (MP = 2-mesitylpyrrolyl, **7**).* A precooled THF (1 mL) solution of **1** (72 mg, 0.23 mmol) was added to a precooled THF (4 mL) solution of sodium 2-mesitylpyrrolide (MP^{Na}) (96 mg, 0.46 mmol) at -78 °C, the flask was rinsed with THF (1 mL) and the solution added to the mixture, which was allowed to warm to r.t. over 20 h. The solvent was evaporated, toluene (1 mL) was added to the residue, and the solvent was evaporated again to remove most of the residual THF. The mixture was extracted with toluene (2 × 2 mL) and the solvent was removed *in vacuo*. Analytically pure material (85 mg, 0.14 mmol, 60%) was obtained by trituration of the solid with hexane (2 × 1 mL). Crystals suitable for X-ray crystallography were grown by storing a concentrated solution of **7** in hexane at -35 °C. ¹H NMR (400 MHz, C₆D₆, 25 °C): δ = 6.83 (bs, 2H, Ar-H), 6.78 (dd, ³J(H,H) = 3.0 Hz, ⁴J(H,H) = 1.5 Hz, 2H, pyrrole-H5), 6.75 (s, 2H, Ar-H), 6.46 (t, ³J(H,H) = 3.0 Hz, 2H, pyrrole-H4), 6.20 (dd, ³J(H,H) = 3.0 Hz, ⁴J(H,H) = 1.5 Hz, 2H, pyrrole-H3), 4.00 (s, 5H, Cp), 2.21 (s, 6H, Ar-CH₃), 2.16 (s, 6H, Ar-CH₃), 2.04 ppm (s, 6H, Ar-CH₃); ¹³C NMR (101 MHz, C₆D₆, 25 °C): δ = 212.1 (CO), 140.5, 139.3, 137.8, 137.3, 132.6, 128.5, 127.9, 126.6, 114.7, 111.5, 85.1 (Cp), 21.9 (Ar-CH₃), 21.7 (Ar-CH₃), 21.2 ppm (Ar-CH₃); ²⁹Si NMR (79 MHz, C₆D₆, 25 °C) δ = 42.6 ppm; IR (THF): $\tilde{\nu}$ = 2027 (CO), 1977 (CO) cm⁻¹; ESI-MS (THF, NEt₄Cl ionizing agent): [M-CO+Cl]⁻: m/z = 615.1183 au, calc'd m/z = 615.1090 au

X-ray Crystal Structure Determination of 7. C₃₃H₃₃ClFeN₂O₂Si, Fw = 609.00, colorless needle, 0.20 × 0.05 × 0.05 mm³, monoclinic, I2/a (no. 15), a = 16.2445(10), b = 12.4009(7), c = 29.225(2) Å, β = 95.498(3)°, V = 5860.3(7) Å³, Z = 8, D_x = 1.381 g/cm³, μ = 0.68 mm⁻¹. 27357 Reflections were measured on a Bruker Kappa ApexII diffractometer with sealed tube and Triumph monochromator (λ = 0.71073 Å) at a temperature of 150(2) K up to a resolution of

($\sin \theta/\lambda$)_{max} = 0.65 Å⁻¹. The Eval15 software¹¹⁰ was used for the intensity integration. A multiscan absorption correction and scaling was performed with SADABS¹¹¹ (correction range 0.61–0.75). 6750 Reflections were unique ($R_{\text{int}} = 0.081$), of which 3828 were observed [$I > 2\sigma(I)$]. The structure was solved with Patterson superposition methods using SHELXT.¹¹² Least-squares refinement was performed with SHELXL-2014¹¹³ against F^2 of all reflections. Non-hydrogen atoms were refined freely with anisotropic displacement parameters. Hydrogen atoms were introduced in calculated positions and refined with a riding model. 367 Parameters were refined with no restraints. $R1/wR2$ [$I > 2\sigma(I)$]: 0.0529/0.1085. $R1/wR2$ [all refl.]: 0.1177/0.1311. $S = 1.010$. Residual electron density between -0.30 and 0.57 e/Å³. Geometry calculations and checking for higher symmetry was performed with the PLATON program.¹¹⁴

Synthesis of (tmim)Na₃ (Na-8). A solution of **8** (4.95 g, 12.3 mmol) in THF (10 mL) was added to prewashed (hexane 3 × 5 mL and THF 5 mL) NaH (60% in oil, 2.07 g, 52 mmol) under THF (20 mL) over 15 min and stirred for 2.75 h. The excess NaH was removed by filtration, and the orange (green luminescent) filtrate was freed of solvent *in vacuo*, yielding a yellow powder (8.46 g, quantitative). Analysis by ¹H NMR showed only (tmim)Na₃ and THF (~30 w%). A titration with HCl (0.1 M in H₂O) on a sample (100.4 mg) in a mixture of THF (4 mL) and water (1 mL) was performed to determine the base content, which was consistent with 68.4 w% (tmim)Na₃. This value was used for stoichiometry calculations in subsequent experiments. ¹H NMR (400 MHz, CD₃CN, 25 °C): $\delta = 7.19$ (m, 6H, ArH), 6.62 (m, 6H, ArH), 6.25 (s, 1H, R₃CH), 2.41 ppm (s, 9H, CH₃). ¹³C NMR (101 MHz, CD₃CN, 25 °C): $\delta = 151.4, 146.0, 132.4, 116.6, 116.2, 115.3, 114.8, 101.8, 37.7$ (R₃CH), 10.1 ppm (CH₃).

Synthesis of (tmim)(C₄H₈O)₃SiFe(CO)₄⁻ Et₄N⁺ (9). A solution of Na-8 (159 mg, 28 w% THF, 0.25 mmol) and NEt₄⁺ (104 mg, 0.240 mmol) in THF (20 mL) was stirred at 60 °C for 72 h. Filtration and evaporation provided 253 mg solid. Precipitation of most of the impurities with Et₂O from THF yielded, after filtration and evaporation of the filtrate, 123 mg material of approximately 70% purity (91.3 μmol, 38%), with minor impurities that could not be identified. ¹H NMR (400 MHz, CD₃CN, 25 °C): $\delta = 7.45$ (d, ³J(H,H) = 8.1 Hz, 3H, indole-H), 7.40 (d, ³J(H,H) = 8.5 Hz, 3H, indole-H), 7.19 (t, ³J(H,H) = 7.7 Hz, 3H, indole-H), 7.06 (t, ³J(H,H) = 7.5 Hz, 3H, indole-H), 6.08 (s, 1H, R₃CH), 4.17–4.04 (m, 3H, N-CH₂ or O-CH₂), 4.04–3.95 (m, 3H, N-CH₂ or O-CH₂), 3.79–3.57 (m, 6H, N-CH₂ or O-CH₂), 3.15 (q, ³J(H,H) = 7.2 Hz, 8H, N(CH₂CH₃)₄), 2.33 (bs, 3H, CH₂), 1.76 (m, 6H, CH₂), 1.61 (m, 3H, CH₂), 1.41 (s, 9H, indole-CH₃), 1.25–1.16 ppm (tt, ³J(H,H) = 7.2 Hz, ³J_{HN} = 1.7 Hz, 12H, N(CH₂CH₃)₄); ¹³C NMR (101 MHz, CD₃CN, 25 °C): $\delta = 220.0$ (CO), 136.6 (indole-C), 132.2 (indole-C), 129.8 (indole-C), 122.6 (indole-CH), 119.7 (indole-CH), 119.2 (indole-CH), 111.1 (indole-C), 110.2 (indole-CH), 61.9 (N-CH₂ or O-CH₂), 53.1 (¹J_{CN} = 3.1 Hz, N(CH₂CH₃)₄), 44.5 (N-CH₂ or O-CH₂), 35.9 (R₃CH), 30.7 (CH₂), 29.1 (CH₂), 7.7 (N(CH₂CH₃)₄), 7.1 ppm (indole-CH₃); IR (ATR): $\tilde{\nu} = 1998, 1903, 1877, 1866$ cm⁻¹.

Synthesis of 2-[(2,6-diisopropylphenyl)iminomethyl]pyrrolide sodium (DippIMP^{Na}). A THF (10 mL) solution of DippIMP^{Na} (766 mg, 3.01 mmol) was added to a suspension of NaHMDS (523 mg, 2.85 mmol) in THF (10 mL) and stirred for 30 min. The solvent was removed *in vacuo* and the solid washed with hexane (3 × 2 mL) and dried *in vacuo* to yield a white powder (803 mg, 18 w% THF, 2.38 mmol, 84%). ¹H NMR (400 MHz, C₆D₆, 25 °C): $\delta = 8.07$ (d, ⁴J(H,H) = 0.9 Hz, 1H, N = CH), 7.45 (q, ³J(H,H) = 1.2 Hz, ⁴J(H,H) = 1.2 Hz, ⁴J(H,H) = 1.2 Hz, 1H, pyrrole-H3), 7.19, 7.13 (AB₂ pattern, $J_{AB} = 7.84$ Hz, 3H, Ar-H), 7.02 (dd, ³J(H,H) = 3.3 Hz, ⁴J(H,H) = 1.2 Hz, 1H, pyrrole-H5), 6.69 (dd, ³J(H,H) = 3.3 Hz, ³J(H,H) = 1.5 Hz, 1H, pyrrole-H4), 3.38 (hept, ³J(H,H) = 6.9 Hz, 2H, iPr-H), 1.22 ppm (d, ³J(H,H) = 6.9 Hz, 12H, iPr-CH₃); ¹³C NMR (101 MHz, C₆D₆ + C₄D₈O, 25 °C): $\delta = 160.4, 151.7, 140.2, 139.3, 136.3, 123.8, 123.4, 120.9, 111.3, 28.2, 24.4$ ppm.

Synthesis of DippIMP–DippAMPsi(Cl)CpFe(CO)₂ (L'–LSi(Cl)Fp, 10). A precooled THF (0.25 mL) solution of DippIMP^{Na} (28 mg, 79 μmol) was added to a precooled THF (1 mL) solution of **1** (12 mg, 39 μmol) at -78 °C, the flask was rinsed with THF (0.25 mL) and the solution added to the mixture, which was allowed to warm to r.t. over 20 h. Evaporation of the solvent *in vacuo*, titration with hexane, and drying *in vacuo* yielded the product (10 mg, 13 μmol, 35%). ¹H NMR (400 MHz, C₆D₆ + C₄D₈O, 25 °C) $\delta = 9.63$ (bs, 1H), 7.61 (bs, 1H, N = CH), 7.34 (dd, ³J(H,H) = 2.6, ⁴J(H,H) = 1.0 Hz, 1H, L-pyrrole-H5), 7.13–7.00 (m, 6H, Ar-H), 6.64 (t, ³J(H,H) = 2.9 Hz, 1H, L-pyrrole-H4), 6.56 (bs, 1H, L'-pyrrole-H), 6.46 (bs, 1H, L'-pyrrole-H), 6.21 (d't, ³J(H,H) = 2.9, ⁴J(H,H) = 1.0 Hz, 1H, L-pyrrole-H3), 5.75 (s, 1H, N-CH), 4.11 (s, 5H, Cp), 3.95 (sept, ³J(H,H) = 6.7 Hz, 1H, L-iPr-H), 3.34 (sept, ³J(H,H) = 6.8 Hz, 1H, L-iPr-H), 3.12 (sept, ³J(H,H) = 6.7 Hz, 2H, L'-iPr-H), 1.38 (d, ³J(H,H) = 6.7 Hz, 3H, L-iPr-CH₃), 1.23 (d, ³J(H,H) = 6.7 Hz, 3H, L-iPr-CH₃), 1.17 (t, ³J(H,H) = 6.7 Hz, 15H, L-iPr-CH₃ + 4L'-iPr-CH₃), 0.60 ppm (d, ³J(H,H) = 6.7 Hz, 3H, L-iPr-CH₃); ¹³C NMR (101 MHz, C₆D₆ + C₄D₈O, 25 °C) $\delta = 213.3$ (CO), 211.3 (CO), 152.4, 150.9, 149.3, 141.6, 139.2, 138.3, 128.7, 127.3, 125.4, 124.4, 124.2, 123.2, 122.7 (L'-pyrrole-CH), 117.1 (L-pyrrole-CS), 116.8 (L'-pyrrole-CH), 115.8 (L-pyrrole-C4), 104.0 (L-pyrrole-C3), 84.3 (Cp), 61.9 (N-CH), 28.9 (L-iPr-CH), 28.3 (L'-iPr-CH), 28.0 (L-iPr-CH), 27.9 (L-iPr-CH₃), 25.6 (L-iPr-CH₃), 25.1 (L-iPr-CH₃), 23.7 (L'-iPr-CH₃), 23.7 ppm (L'-iPr-CH₃); ²⁹Si NMR (79 MHz, C₆D₆ + C₄D₈O, 25 °C) $\delta = 39.4$ ppm.

X-ray Crystal Structure Determination of 10. C₄₁H₄₇ClFeN₄O₂Si · 1.25C₆H₁₄. Fw = 854.93, yellow needle, 0.33 × 0.18 × 0.13 mm³, monoclinic, $P2_1/c$ (no. 14), $a = 10.3742(4)$, $b = 32.3412(10)$, $c = 14.5247(5)$ Å, $\beta = 94.203(2)^\circ$, $V = 4860.2(3)$ Å³, $Z = 4$, $D_x = 1.168$ g/cm³, $\mu = 0.43$ mm⁻¹. 84630 Reflections were measured on a Bruker Kappa ApexII diffractometer with sealed tube and Triumph monochromator ($\lambda = 0.71073$ Å) at a temperature of 150(2) K up to a resolution of ($\sin \theta/\lambda$)_{max} = 0.65 Å⁻¹. The Eval15 software¹¹⁰ was used for the intensity integration. A multiscan absorption correction and scaling was performed with SADABS¹¹¹ (correction range 0.68–0.75). 11158 Reflections were unique ($R_{\text{int}} = 0.036$), of which 8504 were observed [$I > 2\sigma(I)$]. The structure was solved with Patterson superposition methods using SHELXT.¹¹² Least-squares refinement was performed with SHELXL-2014¹¹³ against F^2 of all reflections. Non-hydrogen atoms were refined freely with anisotropic displacement parameters. Hydrogen atoms were introduced in calculated positions and refined with a riding model. The isopropyl group was refined with a model for orientational disorder. There is a cocrystallized *n*-hexane molecule on a general position which was refined with a disorder model. Another *n*-hexane molecule is disordered on an inversion center and was refined with partial occupancy. 639 parameters were refined with 460 restraints (concerning distances, angles, and displacement parameters in the disordered parts). $R1/wR2$ [$I > 2\sigma(I)$]: 0.0521/0.1550. $R1/wR2$ [all refl.]: 0.0714/0.1703. $S = 1.076$. Residual electron density between -0.34 and 0.91 e/Å³. Geometry calculations and checking for higher symmetry was performed with the PLATON program.¹¹⁴

■ ASSOCIATED CONTENT

Supporting Information

The Supporting Information is available free of charge on the ACS Publications website at DOI: 10.1021/acs.organomet.8b00399.

Spectroscopic data and computational details (PDF)

Coordinates of the computed structures (XYZ)

Accession Codes

CCDC 1847861–1847863 contain the supplementary crystallographic data for this paper. These data can be obtained free of charge via www.ccdc.cam.ac.uk/data_request/cif, or by emailing data_request@ccdc.cam.ac.uk, or by contacting The Cambridge Crystallographic Data Centre, 12 Union Road, Cambridge CB2 1EZ, UK; fax: +44 1223 336033.

AUTHOR INFORMATION

Corresponding Author

*E-mail: M.Moret@uu.nl.

ORCID

Marc-Etienne Moret: 0000-0002-3137-6073

Notes

The authors declare no competing financial interest.

ACKNOWLEDGMENTS

Support with the NMR spectroscopic analysis by Dr. J.T.B.H. Jastrzebski is gratefully acknowledged. We acknowledge funding from the European Union Seventh Framework Programme (FP7/2007–2013) under grant agreement PIFI-GA-2012-327306 (IIF-Marie Curie grant awarded to M.E.M.), the Dutch National Research School Combination Catalysis (NRSC-C), and the Sectorplan Natuur- en Scheikunde (Tenure-track grant at Utrecht University). This work was sponsored by NWO Exacte en Natuurwetenschappen (Physical Sciences) for the use of supercomputer facilities, with financial support from The Netherlands Organization for Scientific Research (NWO). The X-ray diffractometer was financed by the NWO.

REFERENCES

- (1) Benedek, Z.; Szilvási, T. Can Low-Valent Silicon Compounds Be Better Transition Metal Ligands than Phosphines and NHCs? *RSC Adv.* **2015**, *5*, 5077–5086.
- (2) Skell, P. S.; Goldstein, E. J. Dimethylsilene: CH_3SiCH_3 . *J. Am. Chem. Soc.* **1964**, *86*, 1442–1443.
- (3) Denk, M.; Lennon, R.; Hayashi, R.; West, R.; Belyakov, A. V.; Verne, H. P.; Haaland, A.; Wagner, M.; Metzler, N. Synthesis and Structure of a Stable Silylene. *J. Am. Chem. Soc.* **1994**, *116*, 2691–2692.
- (4) Blom, B.; Stoelzel, M.; Driess, M. New Vistas in N-Heterocyclic Silylene (NHSi) Transition-Metal Coordination Chemistry: Syntheses, Structures and Reactivity towards Activation of Small Molecules. *Chem. - Eur. J.* **2013**, *19*, 40–62.
- (5) Asay, M.; Jones, C.; Driess, M. N-Heterocyclic Carbene Analogues with Low-Valent Group 13 and Group 14 Elements: Syntheses, Structures, and Reactivities of a New Generation of Multitalented Ligands. *Chem. Rev.* **2011**, *111*, 354–396.
- (6) Sen, S. S.; Khan, S.; Samuel, P. P.; Roesky, H. W. Chemistry of Functionalized Silylenes. *Chem. Sci.* **2012**, *3*, 659–682.
- (7) Zybilla, C.; Müller, G. Synthesis and Structure of $[(\text{OC})_4\text{Fe} = \text{Si}(\text{OtBu})_2\text{-HMPT}]$, a Donor-Stabilized Silanediyl (“Silylene”) Complex. *Angew. Chem., Int. Ed. Engl.* **1987**, *26*, 669–670.
- (8) Raoufoghaddam, S.; Zhou, Y. P.; Wang, Y.; Driess, M. N-Heterocyclic Silylenes as Powerful Steering Ligands in Catalysis. *J. Organomet. Chem.* **2017**, *829*, 2–10.
- (9) Zhang, M.; Liu, X.; Shi, C.; Ren, C.; Ding, Y.; Roesky, H. W. The Synthesis of $(\eta^3\text{-C}_3\text{H}_5)\text{Pd}\{\text{Si}[\text{N}(\text{tBu})\text{CH}_2]_2\}\text{Cl}$ and the Catalytic Property for Heck Reaction. *Z. Anorg. Allg. Chem.* **2008**, *634*, 1755–1758.
- (10) Blom, B.; Gallego, D.; Driess, M. N-Heterocyclic Silylene Complexes in Catalysis: New Frontiers in an Emerging Field. *Inorg. Chem. Front.* **2014**, *1*, 134–148.
- (11) Fürstner, A.; Krause, H.; Lehmann, C. W. Preparation, Structure and Catalytic Properties of a Binuclear Pd(0) Complex with Bridging Silylene Ligands. *Chem. Commun.* **2001**, *80*, 2372–2373.
- (12) Troadec, T.; Prades, A.; Rodriguez, R.; Mirgalet, R.; Baceiredo, A.; Saffon-Merceron, N.; Branchadell, V.; Kato, T. Silacyclopropylideneplatinum(0) Complex as a Robust and Efficient Hydrosilylation Catalyst. *Inorg. Chem.* **2016**, *55*, 8234–8240.
- (13) Zhou, Y. P.; Raoufoghaddam, S.; Szilvási, T.; Driess, M. A Bis(silylene)-Substituted ortho-Carborane as a Superior Ligand in the Nickel-Catalyzed Amination of Arenes. *Angew. Chem., Int. Ed.* **2016**, *55*, 12868–12872.
- (14) Wang, Y.; Kostenko, A.; Yao, S.; Driess, M. Divalent Silicon-Assisted Activation of Dihydrogen in a Bis(N-heterocyclic silylene)-xanthene Nickel(0) Complex for Efficient Catalytic Hydrogenation of Olefins. *J. Am. Chem. Soc.* **2017**, *139*, 13499–13506.
- (15) Ren, H.; Zhou, Y. P.; Bai, Y.; Cui, C.; Driess, M. Cobalt-Catalyzed Regioselective Borylation of Arenes: N-Heterocyclic Silylene as an Electron Donor in the Metal-Mediated Activation of C-H Bonds. *Chem. - Eur. J.* **2017**, *23*, 5663–5667.
- (16) Bai, Y.; Zhang, J.; Cui, C. An arene-tethered silylene ligand enabling reversible dinitrogen binding to iron and catalytic silylation. *Chem. Commun.* **2018**, *54*, 8124–8127.
- (17) Li, H.; Hope-Weeks, L. J.; Krempner, C. A Supramolecular Approach to Zwitterionic Alkaline Metal Silanides and Formation of Heterobimetallic Silanides. *Chem. Commun.* **2011**, *47*, 4117–4119.
- (18) Li, H.; Hung-Low, F.; Krempner, C. Synthesis and Structure of Zwitterionic Silyborates and Silylzincates with Pendant Polydonor Arms. *Organometallics* **2012**, *31*, 7117–7124.
- (19) McNerney, B.; Whittlesey, B.; Krempner, C. Synthesis and Reactivity of New Pyrazolyl-Functionalized Potassium Silanides. *Eur. J. Inorg. Chem.* **2011**, *2011*, 1699–1702.
- (20) Styra, S.; González-Gallardo, S.; Armbruster, F.; Oña-Burgos, P.; Moos, E.; Vonderach, M.; Weis, P.; Hampe, O.; Grün, A.; Schmitt, Y.; Gerhards, M.; Menges, F.; Gaffga, M.; Niedner-Schatteburg, G.; Breher, F. Heterobimetallic Cuprates Consisting of a Redox-Switchable, Silicon-Based Metalloligand: Synthesis, Structures, and Electronic Properties. *Chem. - Eur. J.* **2013**, *19*, 8436–8446.
- (21) Simon, M.; Breher, F. Multidentate silyl ligands in transition metal chemistry. *Dalton Trans.* **2017**, *46*, 7976–7997.
- (22) Murphy, L. J.; Hollenhorst, H.; McDonald, R.; Ferguson, M.; Lumsden, M. D.; Turculet, L. Selective Ni-Catalyzed Hydroboration of CO_2 to the Formaldehyde Level Enabled by New PSiP Ligation. *Organometallics* **2017**, *36*, 3709–3720.
- (23) Metsänen, T. T.; Gallego, D.; Szilvási, T.; Driess, M.; Oestreich, M. Peripheral Mechanism of a Carbonyl Hydrosilylation Catalysed by an SiNSi Iron Pincer Complex. *Chem. Sci.* **2015**, *6*, 7143–7149.
- (24) Vicent, C.; Mas-marza, E.; Sanau, M.; Peris, E. Electrospray Ionization Mass Spectrometry Studies on the Mechanism of Hydrosilylation of Terminal Alkynes Using an N-Heterocyclic Carbene Complex of Iridium, Allow Detection/Characterization of All Reaction Intermediates. *Organometallics* **2006**, *25*, 3713–3720.
- (25) Roy, A. K.; Taylor, R. B. The First Alkene-Platinum-Silyl Complexes: Lifting the Hydrosilylation Mechanism Shroud with Long-Lived Precatalytic Intermediates and True Pt Catalysts. *J. Am. Chem. Soc.* **2002**, *124*, 9510–9524.
- (26) Sekiguchi, A.; Lee, V. Y.; Nanjo, M. Lithiosilanes and Their Application to the Synthesis of Polysilane Dendrimers. *Coord. Chem. Rev.* **2000**, *210*, 11–45.
- (27) Tamao, K.; Kawachi, A. Silyl Anions. *Adv. Organomet. Chem.* **1995**, *38*, 1–58.
- (28) Lickiss, P. D.; Smith, C. M. Silicon Derivatives of the Metals of Groups 1 and 2. *Coord. Chem. Rev.* **1995**, *145*, 75–124.
- (29) Kleeberg, C.; Cascarano, G.; Giacomazzo, C.; Guagliardi, A.; Nudelman, A.; Stoltz, B. M.; Bercaw, J. E.; Goldberg, K. I. On the Structural Diversity of $[\text{K}(18\text{-Crown-6})\text{EPh}_3]$ Complexes (E = C, Si, Ge, Sn, Pb): Synthesis, Crystal Structures and NOESY NMR Study. *Dalton Trans.* **2013**, *42*, 8276–8287.
- (30) Präsang, C.; Scheschke, D. Silyl Anions. *Struct. Bonding (Berlin, Ger.)* **2013**, *156*, 1–47.
- (31) Schwarze, N.; Steinhauer, S.; Neumann, B.; Stammeler, H.-G.; Hoge, B. The Tris(Pentafluoroethyl)Silanide Anion. *Angew. Chem., Int. Ed.* **2016**, *55*, 16156–16160.
- (32) Armbruster, F.; Fernández, I.; Breher, F. Syntheses, Structures, and Reactivity of Poly(Pyrazolyl)Silanes, -Disilanes, and the Ambidentate $\kappa^1\text{Si}/\kappa^3\text{N}$ -Coordinating Tris(3,5-Dimethylpyrazolyl)-Silanide Ligand $[\text{Si}(3,5\text{-Me}_2\text{pz})_3]^-$ (MeTpsd). *Dalton Trans.* **2009**, *29*, 5612–5626.

- (33) Witteman, L.; Evers, T.; Lutz, M.; Moret, M. A Free Silanide from Nucleophilic Substitution at Silicon(II). *Chem. - Eur. J.* **2018**, *24*, 12236–12240.
- (34) Li, H.; Aquino, A. J. A.; Cordes, D. B.; Hase, W. L.; Krempner, C. Electronic Nature of Zwitterionic Alkali Metal Methanides, Silanides and Germanides - A Combined Experimental and Computational Approach. *Chem. Sci.* **2017**, *8*, 1316–1328.
- (35) Korogodsky, G.; Bendikov, M.; Bravo-Zhivotovskii, D.; Apeloig, Y. Determination of the Solution Acidity of Tris-(Trimethylsilyl) Silane. *Organometallics* **2002**, *21*, 3157–3161.
- (36) Turnblom, E. W.; Boettcher, R. J.; Mislaw, K. Synthesis and Lithiation of Ortho-Methylated Triphenylsilanes. *J. Am. Chem. Soc.* **1975**, *97*, 1766–1772.
- (37) Becker, B.; Corriu, R. J. P.; Guérin, C.; Henner, B. J. L. Hypervalent Silicon Hydrides: Evidence for Their Intermediacy in the Exchange Reactions of Di- and Tri-Hydrogenosilanes Catalysed by Hydrides (NaH, KH and LiAlH₄). *J. Organomet. Chem.* **1989**, *369*, 147–154.
- (38) Graham, W. A. G.; Jetz, W. Silicon-Transition Metal Chemistry. I. Photochemical Preparation of Silyl(Transition Metal) Hydrides. *Inorg. Chem.* **1971**, *10*, 4–9.
- (39) Corey, J. Y.; Braddock-Wilking, J. Reactions of Hydrosilanes with Transition-Metal Complexes: Formation of Stable Transition-Metal Silyl Compounds. *Chem. Rev.* **1999**, *99*, 175–292.
- (40) Corey, J. Y. Reactions of Hydrosilanes with Transition Metal Complexes. *Chem. Rev.* **2016**, *116*, 11291–11435.
- (41) Hübler, K.; Roper, W. R.; Wright, L. J. Tri-N-Pyrrolylsilyl Complexes of Ruthenium and Osmium. *Organometallics* **1997**, *16*, 2730–2735.
- (42) Bentham, J. E.; Cradock, S.; Ebsworth, E. A. V. Silyl and Germyl Compounds of Platinum and Palladium. Part I. Platinum Derivatives of Monosilane and Monogermane. *J. Chem. Soc. A* **1971**, 587–593.
- (43) Clark, H. C.; Rake, A. T. Reactivity of Metal-Metal Bonds XII. The Preparation of Some Phenylchloro Group IVB Derivatives of Pentacarbonylmanganese and (Pi-Cyclo-Pentadienyl)Dicarbonyliron and Their Reactivities towards Pentafluorophenyllithium. *J. Organomet. Chem.* **1974**, *74*, 29–42.
- (44) Höfler, M.; Scheuren, J.; Weber, G. Austauschreaktionen an Komplexgebundenen Liganden von Elementen Der IV. Hauptgruppe. *J. Organomet. Chem.* **1974**, *78*, 347–355.
- (45) Thum, G.; Malisch, W. Synthese Und Reaktivität von Silicium-Übergangsmetall-Komplexen. *J. Organomet. Chem.* **1984**, *264*, C5–C9.
- (46) Choe, S.-B.; Schneider, J. J.; Klabunde, K. J.; Radonovich, L. J.; Ballantine, T. A. New Silyl-Nickel Complexes Prepared by η⁶-Arene Substitution in (η⁶-Toluene)Bis(Trihalosilyl)Nickel. Preparation of L₂Ni(SiX₃)₂ and L₂Ni(SiX₃)₂ (X = Cl, F; L = Phosphine, Phosphites, and Pyridines. X-Ray Structure of Cis-(Collidine)₂Si(SiCl₃)₂. *J. Organomet. Chem.* **1989**, *376*, 419–439.
- (47) Albrecht, M.; Kwok, W. H.; Lu, G. L.; Rickard, C. E. F.; Roper, W. R.; Salter, D. M.; Wright, L. J. Osmadisiloxane and Osmastannasiloxane Complexes Derived from Silanolate Complexes of Osmium(II). *Inorg. Chim. Acta* **2005**, *358*, 1407–1419.
- (48) Clark, G. R.; Lu, G.-L.; Rickard, C. E. F.; Roper, W. R.; Wright, L. J. Metallocyclic Complexes with Ortho-Silylated Triphenylphosphine Ligands, LnOs(κ²(Si,P)-SiMe₂C₆H₄PPh₂)₂, Derived from Thermal Reactions of the Coordinatively Unsaturated Trimethylsilyl Methyl Complex, Os(SiMe₃)(Me)(CO)(PPh₃)₂. *J. Organomet. Chem.* **2005**, *690*, 3309–3320.
- (49) Möller, S.; Fey, O.; Malisch, W.; Seelbach, W. Metallo-silanole und Metallo-siloxane VII. Zur Oxofunktionalisierung von Rutheniohydrosilanen mit Dimethyldioxiran: Darstellung der ersten Ruthenio-silanole. *J. Organomet. Chem.* **1996**, *507*, 239–244.
- (50) Hübler, K.; Hunt, P. A.; Maddock, S. M.; Rickard, C. E. F.; Roper, W. R.; Salter, D. M.; Schwerdtfeger, P.; Wright, L. J. Examination of Metal-Silicon Bonding through Structural and Theoretical Studies of an Isostructural Set of Five-Coordinate Silyl Complexes, Os(SiR₃)Cl(CO)(PPh₃)₂ (R = F, Cl, OH, Me). *Organometallics* **1997**, *16*, 5076–5083.
- (51) Kwok, W. H.; Lu, G. L.; Rickard, C. E. F.; Roper, W. R.; Wright, L. J. Nucleophilic Substitution Reactions at the Si-Cl Bonds of the Dichloro(Methyl)Silyl Ligand in Five- and Six-Coordinate Complexes of Ruthenium(II) and Osmium(II). *J. Organomet. Chem.* **2004**, *689*, 2511–2522.
- (52) Freeman, S. T. N.; Lofton, L. L.; Lemke, F. R. Effect (or Lack Thereof) of Ancillary Groups on the Preparation and Spectroscopic Properties of Ruthenium Silyl Complexes Containing the Cp-(PR₃)₂Ru Moiety. *Organometallics* **2002**, *21*, 4776–4784.
- (53) Malisch, W.; Kuhn, M. Halogenierung Übergangsmetall-Substituierter Hydrosilane. *Chem. Ber.* **1974**, *107*, 2835–2851.
- (54) Wachtler, U.; Malisch, W.; Kolba, E.; Matreux, J. Synthese Und Reaktivität von Silicium-Übergangsmetall-Komplexen XXI*. Ferrio-Azidosilane and Ferriosilyl-Iminophosphorane. *J. Organomet. Chem.* **1989**, *363*, C36–C40.
- (55) Kertsus-Banchik, E.; Kalikhman, I.; Gostevskii, B.; Deutsch, Z.; Botoshansky, M.; Kost, D. Hydride Migration from Silicon to an Adjacent Unsaturated Imino Carbon: Intramolecular Hydrosilylation. *Organometallics* **2008**, *27*, 5285–5294.
- (56) Novák, M.; Dostál, L.; Alonso, M.; De Proft, F.; Růžicka, A.; Lyčka, A.; Jambor, R. Hydrosilylation Induced by N→Si Intramolecular Coordination: Spontaneous Transformation of Organosilanes into 1-Aza-Silole-Type Molecules in the Absence of a Catalyst. *Chem. - Eur. J.* **2014**, *20*, 2542–2550.
- (57) Witteman, L.; Evers, T.; Shu, Z.; Lutz, M.; Klein Gebbink, R. J. M.; Moret, M.-E. Hydrosilylation in Aryliminopyrrolide-Substituted Silanes. *Chem. - Eur. J.* **2016**, *22*, 6087–6099.
- (58) Fester, G. W.; Eckstein, J.; Gerlach, D.; Brendler, E.; Kroke, E. Reactions of Hydridochlorosilanes with 2,2'-Bipyridine and 1,10-Phenanthroline: Complexation versus Dismutation and Metal-Catalyst-Free 1,4-Hydrosilylation. *Inorg. Chem.* **2010**, *49*, 2667–2673.
- (59) Lippe, K.; Gerlach, D.; Kroke, E.; Wagler, J. Hypercoordinate Organosilicon Complexes of an ONN'O' Chelating Ligand: Regio- and Diastereoselectivity of Rearrangement Reactions in Si–Salphen Systems. *Organometallics* **2009**, *28*, 621–629.
- (60) Novák, M.; Dostál, L.; Turek, J.; Alonso, M.; De Proft, F.; Růžicka, A.; Jambor, R. Spontaneous Double Hydrometallation Induced by N→M Coordination in Organometallic Hydrides of Group 14 Elements. *Chem. - Eur. J.* **2016**, *22*, S620–S628.
- (61) Novák, M.; Hošnová, H.; Dostál, L.; Glowacki, B.; Jurkschat, K.; Lyčka, A.; Ruzickova, Z.; Jambor, R. Hydrosilylation of RN=CH Imino-Substituted Pyridines without a Catalyst. *Chem. - Eur. J.* **2017**, *23*, 3074–3083.
- (62) Connolly, J. W.; Hatlee, M. J.; Cowley, A. H.; Sharp, P. R. Variable Temperature ¹³C NMR Study of Some L(CO)₃FeH(SiR₃) (L = CO, P(OPh)₃; R = Ph, Me, Cl) Species. X-Ray Crystal Structure Of P(OPh)₃(CO)₃Fe(H)SiPh₃. *Polyhedron* **1991**, *10*, 841–849.
- (63) Udovich, C. A.; Clark, R. J.; Haas, H. Stereochemical Nonrigidity in Iron Carbonyl Fluorophosphine Compounds. *Inorg. Chem.* **1969**, *8*, 1066–1072.
- (64) Mann, B. E. Measurement of the Coupling Constants ¹J(⁵⁷Fe–¹³C) and ¹J(⁵⁷Fe–³¹P) in Phosphine and Carbonyl Complexes of Iron. *J. Chem. Soc. D* **1971**, *0*, 1173–1174.
- (65) Shapley, J. R.; Osborn, J. A. Rapid Intramolecular Rearrangements in Pentacoordinate Transition Metal Compounds. *Acc. Chem. Res.* **1973**, *6*, 305–312.
- (66) Rossi, A. R.; Hoffmann, R. Transition Metal Pentacoordination. *Inorg. Chem.* **1975**, *14*, 365–374.
- (67) Whitmire, K. H.; Lee, T. R. Carbon-13 NMR Studies of Some Iron Carbonyls: An Unexpected Trend in the Chemical Shifts of Disubstituted Complexes. *J. Organomet. Chem.* **1985**, *282*, 95–106.
- (68) Gansow, O. A.; Burke, A. R.; Vernon, W. D. Temperature-Dependent Carbon-13 Nuclear Magnetic Resonance Spectra of the η⁵-Cyclopentadienyliron Dicarbonyl Dimer, an Application of a Shiftless Relaxation Reagent. *J. Am. Chem. Soc.* **1972**, *94*, 2550–2552.
- (69) Cotton, F. A.; Troup, J. M. Reactivity of Diiron Nonacarbonyl in Tetrahydrofuran. I. Isolation and Characterization of Pyridinete-

tracarbonyliron and Pyrazinetetracarbonyliron. *J. Am. Chem. Soc.* **1974**, *96*, 3438–3443.

(70) Jesson, J. P.; Meakin, P. Nuclear Magnetic Resonance Evidence for Stereochemical Rigidity in ML_5 Complexes. *J. Am. Chem. Soc.* **1973**, *95*, 1344–1346.

(71) Howell, J. A. S.; Palin, M. G.; McArdle, P.; Cunningham, D.; Goldschmidt, Z.; Gottlieb, H. E.; Hezroni-Langerman, D. Influence of Phosphine Conformation on the Structure and Stereodynamics of Tetracarbonyl(Tri-*o*-Tolylphosphine)Iron and Pentacarbonyl(Tri-*o*-Tolylphosphine)Chromium. *Inorg. Chem.* **1991**, *30*, 4683–4685.

(72) Howell, J. A. S.; Palin, M. G.; McArdle, P.; Cunningham, D.; Goldschmidt, Z.; Gottlieb, H. E.; Hezroni-Langerman, D. Structure and Stereodynamics of Iron Carbonyl Phosphine or Arsinic $Fe(CO)_4L$ Complexes ($L = P(o-Tolyl)_3$, $As(o-Tolyl)_3$, $P(o-Tolyl)_2CH_2Ph$, $(o-Tolyl)_2PP(o-Tolyl)_2$). *Inorg. Chem.* **1993**, *32*, 3493–3500.

(73) Barnard, T. S.; Mason, M. R. Hindered Axial–Equatorial Carbonyl Exchange in an $Fe(CO)_4(PR_3)$ Complex of a Rigid Bicyclic Phosphine. *Inorg. Chem.* **2001**, *40*, 5001–5009.

(74) Graham, W. a. G.; Jetz, W. Silicon-Transition Metal Chemistry. II. Anions Derived from Silyl(Transition Metal) Hydrides and Related Compounds. *Inorg. Chem.* **1971**, *10*, 1647–1653.

(75) Breit, N. C.; Eisenhut, C.; Inoue, S. Phosphinosilylenes as a Novel Ligand System for Heterobimetallic Complexes. *Chem. Commun.* **2016**, *52*, 5523–5526.

(76) Corey, J. Y.; Chang, L. S.; Corey, E. R. Dehydrogenative Coupling of Heterocyclic Dihydrosilanes. *Organometallics* **1987**, *6*, 1595–1596.

(77) Chang, L. S.; Corey, J. Y. Dehydrogenative Coupling of Diarylsilanes. *Organometallics* **1989**, *8*, 1885–1893.

(78) Zybilla, C.; Mueller, G. Synthesis and Structure of the Donor-Stabilized Silylene (Silanediyl) Complexes $(t-C_4H_9O)_2Si = Cr(CO)_5$, HMPt and $(t-C_4H_9O)_2Si = Fe(CO)_4$ HMPt. *Organometallics* **1988**, *7*, 1368–1372.

(79) Leis, C.; Wilkinson, D. L.; Handwerker, H.; Zybilla, C.; Mueller, G. Structure and Photochemistry of New Base-Stabilized Silylene (Silanediyl) Complexes $R_2(HMPA)Si=M(CO)_n$ of Iron, Chromium, and Tungsten ($R = t-BuO$, $t-BuS$, $MesO$, $1-AdaO$, $2-AdaO$, $NeopO$, $TritO$, Me , Cl ; $M = Fe$, $n = 4$; $M = Cr$, W , $n = 5$): Sila-Wittig Reaction of the Base-Free Reactive Intermediate $[Me_2Si = Cr(CO)_5]$. *Organometallics* **1992**, *11*, 514–529.

(80) Zybilla, C.; Wilkinson, D. L.; Leis, C.; Müller, G. Identification of $[(OC)_4Fe = Si(CH_3)_2\{(H_3C)_2N\}_3PO]$ as Intermediate in the Formation of Polysilanes from $(H_3C)_2SiCl_2$ and $[Na_2Fe(CO)_4]$. *Angew. Chem., Int. Ed. Engl.* **1989**, *28*, 203–205.

(81) Ghadwal, R. S.; Azhakar, R.; Pröpper, K.; Holstein, J. J.; Ditttrich, B.; Roesky, H. W. Heterocyclic Carbene Stabilized Dichlorosilylene Transition-Metal Complexes of V(I), Co(I), and Fe(0). *Inorg. Chem.* **2011**, *50*, 8502–8508.

(82) Leis, C.; Zybilla, C.; Lachmann, J.; Müller, G. Silylene Complexes Stabilized by Sulphur Substituents; a Structure and Reactivity Study. *Polyhedron* **1991**, *10*, 1163–1171.

(83) Lang, H.; Weinmann, M.; Frosch, W.; Büchner, M.; Schiemenz, B. Novel Inter- and Intra-Molecular Donor-Stabilized 1-Metalla-2-Sila-1,3-Dienes. *Chem. Commun.* **1996**, *26*, 1299–1300.

(84) Simons, R. S.; Galat, K. J.; Bradshaw, J. D.; Youngs, W. J.; Tessier, C. A.; Aullón, G.; Alvarez, S. Reaction Chemistry, NMR Spectroscopy, and X-Ray Crystallography of $[Fe_2(\mu-SiMe_2)(CO)_4]$ and $[Fe_2(\mu-SiMeCl)(CO)_4]$. Electronic Structure and Bonding in Fe_2E_2 Rings of $[Fe_2(\mu-ER_2)(CO)_4]$ Binuclear Complexes ($E = C, Si, Ge, Sn, Pb$). *J. Organomet. Chem.* **2001**, *628*, 241–254.

(85) Braunstein, P.; Veith, M.; Blin, J.; Huch, V. New Mono- and Polynuclear Iron Silylene and Stannylenes Complexes. *Organometallics* **2001**, *20*, 627–633.

(86) Schmedake, T. A.; Haaf, M.; Paradise, B. J.; Millevolte, A. J.; Powell, D. R.; West, R. Electronic and Steric Properties of Stable Silylene Ligands in Metal(0) Carbonyl Complexes. *J. Organomet. Chem.* **2001**, *636*, 17–25.

(87) Weinmann, M.; Rheinwald, G.; Zsolnai, L.; Walter, O.; Büchner, M.; Schiemenz, B.; Huttner, G.; Lang, H. New

Investigations in Silanediyl Complex Chemistry: Synthesis, Structure, and Bonding of 1-Metalla-2-Sila-1,3-Dienes. *Organometallics* **1998**, *17*, 3299–3307.

(88) Lutters, D.; Severin, C.; Schmidtman, M.; Müller, T. Activation of 7-Silanorbornadienes by N-Heterocyclic Carbenes: A Selective Way to N-Heterocyclic-Carbene-Stabilized Silylenes. *J. Am. Chem. Soc.* **2016**, *138*, 6061–6067.

(89) Simons, R. S.; Tessier, C. A. $[Fe_2(CO)_4(PMe_3)_4(\mu-H)(\mu-SiCl_2)][Fe(CO)_4(SiCl_3)]$. *Acta Crystallogr., Sect. C: Cryst. Struct. Commun.* **1996**, *52*, 840–842.

(90) Junold, K.; Baus, J. A.; Burschka, C.; Vent-Schmidt, T.; Riedel, S.; Tacke, R. Five-Coordinate Silicon(II) Compounds with Si–M Bonds ($M = Cr, Mo, W, Fe$): Bis[N, N' -Diisopropylbenzamidinato(–)]Silicon(II) as a Ligand in Transition-Metal Complexes. *Inorg. Chem.* **2013**, *52*, 11593–11599.

(91) Tacke, R.; Kobelt, C.; Baus, J. A.; Bertermann, R.; Burschka, C. Synthesis, Structure and Reactivity of a Donor-Stabilised Silylene with a Bulky Bidentate Benzamidinato Ligand. *Dalton Trans.* **2015**, *44*, 14959–14974.

(92) Blom, B.; Pohl, M.; Tan, G.; Gallego, D.; Driess, M. From Unsymmetrically Substituted Benzamidinato and Guanidinato Dichlorohydrosilanes to Novel Hydrido N-Heterocyclic Silylene Iron Complexes. *Organometallics* **2014**, *33*, 5272–5282.

(93) Mück, F. M.; Kloß, D.; Baus, J. a.; Burschka, C.; Tacke, R. Novel Transition-Metal ($M = Cr, Mo, W, Fe$) Carbonyl Complexes with Bis(Guanidinato)Silicon(II) Ligands. *Chem. - Eur. J.* **2014**, *20*, 9620–9626.

(94) Yang, W.; Fu, H.; Wang, H.; Chen, M.; Ding, Y.; Roesky, H. W.; Jana, A. A Base-Stabilized Silylene with a Tricoordinate Silicon Atom as a Ligand for a Metal Complex. *Inorg. Chem.* **2009**, *48*, 5058–5060.

(95) Du, V. A.; Baumann, S. O.; Stipicic, G. N.; Schubert, U. Z. *Naturforsch., B: J. Chem. Sci.* **2009**, *64b*, 1553–1557.

(96) Pfister, H.; Fenske, D. *Z. Anorg. Allg. Chem.* **2001**, *627*, 575–582.

(97) Cordero, B.; Gómez, V.; Platero-Prats, A. E.; Revés, M.; Echeverría, J.; Cremades, E.; Barragán, F.; Alvarez, S. Covalent Radii Revisited. *Dalton Trans.* **2008**, *No. 21*, 2832–2838.

(98) Frisch, M. J.; Trucks, G. W.; Schlegel, H. B.; Scuseria, G. E.; Robb, M. A.; Cheeseman, J. R.; Scalmani, G.; Barone, V.; Mennucci, B.; Petersson, G. A.; Nakatsuji, H.; Caricato, M.; Li, X.; Hratchian, H. P.; Izmaylov, A. F.; Bloino, J.; Zheng, G.; Sonnenberg, J. L.; Hada, M.; Ehara, M.; Toyota, K.; Fukuda, R.; Hasegawa, J.; Ishida, M.; Nakajima, T.; Honda, Y.; Kitao, O.; Nakai, H.; Vreven, T.; Montgomery, J. A., Jr.; Peralta, J. E.; Ogliaro, F.; Bearpark, M.; Heyd, J. J.; Brothers, E.; Kudin, K. N.; Staroverov, V. N.; Keith, T.; Kobayashi, R.; Normand, J.; Raghavachari, K.; Rendell, A.; Burant, J. C.; Iyengar, S. S.; Tomasi, J.; Cossi, M.; Rega, N.; Millam, J. M.; Klene, M.; Knox, J. E.; Cross, J. B.; Bakken, V.; Adamo, C.; Jaramillo, J.; Gomperts, R.; Stratmann, R. E.; Yazyev, O.; Austin, A. J.; Cammi, R.; Pomelli, C.; Ochterski, J. W.; Martin, R. L.; Morokuma, K.; Zakrzewski, V. G.; Voth, G. A.; Salvador, P.; Dannenberg, J. J.; Dapprich, S.; Daniels, A. D.; Farkas, O.; Foresman, J. B.; Ortiz, J. V.; Cioslowski, J.; Fox, D. J. *Gaussian 09*, Revision D.01; Gaussian, Inc.: Wallingford, CT, 2013.

(99) Bent, H. A. An Appraisal of Valence-Bond Structures and Hybridization in Compounds of the First-Row Elements. *Chem. Rev.* **1961**, *61*, 275–311.

(100) Ernst, C. R.; Spialter, L.; Buell, G. R.; Wilhite, D. L. Silicon-29 Nuclear Magnetic Resonance. Chemical Shift Substituent Effects. *J. Am. Chem. Soc.* **1974**, *96*, 5375–5381.

(101) von Döbeneck, H.; Prieztel, H. Further Observations on Reaction between Aldehydes and Indole Derivatives. *Hoppe-Seyler's Z. Physiol. Chem.* **1955**, *299*, 214–226.

(102) Okazaki, M.; Iwata, M.; Tobita, H.; Ogino, H. Reactions of $M[(\eta^5-C_5Me_5)Fe(CO)_2]$ with $ClSiMe_2NR_2$ in THF, Et_2O and Toluene ($M = Li$ and K ; $R = Me, Et, iPr$ and Ph). *Dalton Trans.* **2003**, *6*, 1114–1120.

(103) Dufour, P.; Dartiguenave, M.; Dartiguenave, Y.; Simard, M.; Beauchamp, A. L. Reactions of 1,1-dichloro-, 1-chloro-1-phenyl- and 1-chloro-1-methylsilacyclopent-3-ene with Na[Cp(CO)₂Fe]. X-Ray Diffraction Study of the 1-(dicarbonylcyclopentadienylferrio)-1-[4-(dicarbonylcyclopentadienylferrio)but-1-oxy]silacyclopent-3-ene Resulting from Insertion of an Opened THF Molecule into a Si–Fe Bond. *J. Organomet. Chem.* **1998**, *563*, 53–60.

(104) Li, Y.-S.; Li, Y.-R.; Li, X.-F. New Neutral Nickel(II) Complexes Bearing Pyrrole-Imine Chelate Ligands: Synthesis, Structure and Norbornene Polymerization Behavior. *J. Organomet. Chem.* **2003**, *667*, 185–191.

(105) Fulmer, G. R.; Miller, A. J. M.; Sherden, N. H.; Gottlieb, H. E.; Nudelman, A.; Stoltz, B. M.; Bercaw, J. E.; Goldberg, K. I. NMR Chemical Shifts of Trace Impurities: Common Laboratory Solvents, Organics, and Gases in Deuterated Solvents Relevant to the Organometallic Chemist. *Organometallics* **2010**, *29*, 2176–2179.

(106) Armarego, W. L. F.; Chai, C. L. L. *Purification of laboratory chemicals*; 2003.

(107) Krentz, R.; Pomeroy, R. K. Silicon-29 NMR Investigation of Silyl Derivatives of the Iron-Group Transition Metals. *Inorg. Chem.* **1985**, *24*, 2976–2980.

(108) Ohishi, T.; Shiotani, Y.; Yamashita, M. A Convenient One-Flask Preparation of Pure Potassium Cyclopentadienyldicarbonylferate, K[η^5 -C₅H₅)Fe(CO)₂]. *J. Org. Chem.* **1994**, *59*, 250–250.

(109) Malisch, W.; Kuhn, M. Die Modifizierte Alkalisaltz-Eliminierungsmethode - Ein Genereller Weg Zu Komplexen Mit Silicium-Übergangsmetall-Struktureinheiten. *Chem. Ber.* **1974**, *107*, 979–995.

(110) Schreurs, A. M. M.; Xian, X.; Kroon-Batenburg, L. M. J. EVAL15: a diffraction data integration method based on ab initio predicted profiles. *J. Appl. Crystallogr.* **2010**, *43*, 70–82.

(111) Sheldrick, G. M. SADABS and TWINABS; Universität Göttingen: Germany, 2014.

(112) Sheldrick, G. M. SHELXT - Integrated space-group and crystal-structure determination. *Acta Crystallogr., Sect. A: Found. Adv.* **2015**, *A71*, 3–8.

(113) Sheldrick, G. M. Crystal structure refinement with SHELXL. *Acta Crystallogr., Sect. C: Struct. Chem.* **2015**, *C71*, 3–8.

(114) Spek, A. L. Structure validation in chemical crystallography. *Acta Crystallogr., Sect. D: Biol. Crystallogr.* **2009**, *D65*, 148–155.